ENVIRONMENTAL RESEARCH LETTERS

PURPOSE-LED PUBLISHING™

Part of the ENVIRONMENTAL RESEARCH SERIES

LETTER • OPEN ACCESS

Soil moisture dominates the severe decline in gross primary productivity during a 2023–2024 compound heatwave-drought event over the Amazon

To cite this article: Te Yang *et al* 2025 *Environ. Res. Lett.* **20** 034024

ENVIRONMENTAL RESEARCH
LETTERS

CrossMark

OPEN ACCESS

RECEIVED
4 November 2024

REVISED
21 January 2025

ACCEPTED FOR PUBLICATION
31 January 2025

PUBLISHED
18 February 2025

LETTER

Soil moisture dominates the severe decline in gross primary productivity during a 2023–2024 compound heatwave-drought event over the Amazon

Te Yang[1], Bin Chen[2,*], Shaoqiang Wang[1,2,*], Xiyan Xu[3,4], Paulo Artaxo[5], Tingyu Li[1], Haoyu Peng[1] and Xin Yu[1,6]

1 School of Geography and Information Engineering, China University of Geosciences, Wuhan, People's Republic of China
2 Key Laboratory of Ecosystem Network Observation and Modeling, Institute of Geographic Sciences and Natural Resources Research, Chinese Academy of Sciences, Beijing, People's Republic of China
3 Key Laboratory of Regional Climate-Environment for Temperate East Asia, Institute of Atmospheric Physics, Chinese Academy of Sciences, Beijing, People's Republic of China
4 Collaborative Innovation Center on Forecast and Evaluation of Meteorological Disasters (CIC-FEMD), Nanjing University of Information Science & Technology, Nanjing, People's Republic of China
5 Institute of Physics, University of São Paulo, Sao Paulo, Brazil
6 World Wide Fund for Nature Beijing Office, Beijing, People's Republic of China
* Authors to whom any correspondence should be addressed.

E-mail: chenbin@igsnrr.ac.cn and sqwang@igsnrr.ac.cn

Keywords: gross primary productivity, compound heatwave-drought, extreme climate event, Amazon

Supplementary material for this article is available online

Abstract

The Amazon, the world's largest tropical forest, plays a critical role in the global carbon cycle. It has a large carbon pool and acts as a major carbon sink. However, in 2023–2024, a compound heatwave-drought (CHWD) event (HD2023) hit the Amazon region, resulting in extreme temperatures and soil moisture deficits, threatening the region's carbon sink capacity. Using advanced multisource satellite data and meteorological reanalysis, we quantified the impact of various climatic factors on vegetation productivity during HD2023 and analyzed its progression. Our findings showed that HD2023 led to a 530 Tg C decline in gross primary productivity (GPP) and 0.003 reduction in near-infrared reflectance of vegetation. The strongest phase of the event spanned 5 months, causing persistently high temperatures and reduced precipitation, leading to a continuous decline in soil moisture and marked reduction in GPP. The most severe decrease in GPP occurred in January 2024. The event originated in the northwest and gradually spread to the southeast. Soil moisture was the dominant factor in the decline of photosynthesis across vegetation types, whereas high solar radiation mitigated the impact of drought in evergreen broad forests and savannas. Moreover, the sensitivity of GPP to CHWD varied across vegetation types, ranking as grassland > savanna > evergreen broad forest. This study assessed the impact of HD2023 on regional carbon flux in the Amazon. As climate projections indicate future increases in climate extremes over the Amazon, it is important to identify the drivers of this impact on the carbon cycle of the Amazon.

1. Introduction

The Amazon, the world's largest tropical rainforest, is crucial to the global carbon cycle, storing approximately 120 Pg of carbon in its biomass, and through photosynthesis and respiration, exchanges 18 Pg C annually (Phillips *et al* 2009). Due to this large carbon pool and flux, the Amazon plays a significant role in the global carbon budget (Pan *et al* 2011, Davidson *et al* 2012, Artaxo *et al* 2022a). The Amazon is susceptible to climate change drivers, particularly increases in temperature and decreases in precipitation, which affect several processes that influence the carbon cycle (Artaxo *et al* 2022a, Artaxo *et al* 2022b, Artaxo 2023, Chen *et al* 2024).

Over the past few decades, the Amazon has been affected by several compound heatwave-drought (CHWD) events, threatening the region's carbon sink capacity. A marked change in the hydrological balance in central Brazil associated with a severe warming trend can be identified starting in the 1970s, which has no analog over the last 720 years (Stríkis *et al* 2024). Other examples include extreme droughts in 2005 and 2010 due to the warming anomaly of the Tropical North Atlantic and the recent 2015–2016 El Niño event (Doughty *et al* 2015, Jiménez-Muñoz *et al* 2016, Yang *et al* 2018, Bennett *et al* 2023). The well-documented intense drought of 2005 shows that during that event, the forest lost between 1.2 and 1.6 Pg of carbon (Phillips *et al* 2009). In the Amazon, forest degradation, rather than fire emissions, was the predominant driver of carbon loss between 2010 and 2020 (Feng *et al* 2024) and the increasing frequency of CHWD events is expected to intensify this trend.

The year 2023 was the hottest year on record, with the global average temperature reaching 1.45 °C above pre-industrial levels (1850–1900) (Perkins-Kirkpatrick *et al* 2024). The El Niño events of 2023–2024 increased the risk of record-breaking regional temperatures (Espinoza *et al* 2024, Jiang *et al* 2024). In 2023–2024, a CHWD event (HD2023) in the Amazon region (Rodrigues 2023) severely affected the livelihoods of local people and the carbon and water cycles of terrestrial ecosystems. Nevertheless, the effects of HD2023 on carbon flux in the Amazon have not been fully investigated.

In recent years, due to anthropogenic greenhouse gas emissions, extreme heatwaves and droughts have occurred more frequently (Ridder *et al* 2022). Drought and heat waves are among the most critical abiotic factors influencing the terrestrial carbon cycle (Perkins *et al* 2012, Zscheischler *et al* 2014). Moreover, the combined impact of heat waves and droughts on ecosystem functioning exceeds the effects of either stress alone, demonstrating the nonlinear amplification of both extremes (Zhu *et al* 2021). CHWD events are characterized by low precipitation and high air temperature, which would significantly reduce soil moisture, cause soil water stress on plant photosynthetic rates, and increase the risk of fire (Littell *et al* 2016). For example, CHWD events in Europe in the summer of 2018 caused carbon sinks in Central Europe and southern Sweden to reach record lows, with carbon dioxide uptake falling by more than 50% (Bastos *et al* 2020). Therefore, a broad and in-depth understanding of plant responses to CHWDs is essential for understanding the global and regional carbon cycles.

Gross primary productivity (GPP) represents the total amount of carbon compounds produced by photosynthesis in an ecosystem over a given period. The GPP has the largest carbon flux, with its variations significantly affecting the entire terrestrial carbon cycle (Chen *et al* 2019b). Owing to the increased frequency of CHWDs, the GPP anomalies of mid-latitude ecosystems in the Northern Hemisphere increased significantly by approximately 10.6% from 2000 to 2016 compared with the period from 1982 to 1998 (Gampe *et al* 2021). A record-breaking CHWD hit China's Yangtze River Basin in the summer of 2022, causing widespread reductions in GPP (Wang *et al* 2023a, Li *et al* 2024a). Extreme events can cause significant reductions in the GPP, severely affecting the carbon sink capacity of terrestrial ecosystems. Consequently, understanding the response of terrestrial GPP to extreme climate events, such as CHWDs, is vital for forecasting how global terrestrial ecosystems will respond to future climate change (Wang *et al* 2018).

Therefore, this study utilized the latest multi-source satellite and meteorological reanalysis datasets to quantify the contribution of various climatic factors to changes in vegetation productivity during HD2023 and analyze the process of HD2023 in the Amazon region (approximately 30° S–15° N and 30° W–85° W). Specifically, we aimed to (1) examine the spatiotemporal variations in climate and photosynthetic anomalies, (2) explore the impact of different climatic factors on the response of photosynthesis to HD2023, and (3) analyze the development of HD2023 and the responses of different vegetation types. The results of this study reveal the potential impact of environmental factors on vegetation photosynthesis and will help deepen the understanding of how the GPP of terrestrial ecosystems in the Amazon has responded to the most severe CHWD since 2000.

2. Data and methods

2.1. ERA5-land reanalysis meteorology data

The 2 m air temperature, precipitation, surface solar radiation downwards, and soil moisture (averaged over depths of 1–100 cm) were adopted from the ERA5-Land dataset (Muñoz-Sabater *et al* 2021). We acquired monthly meteorological data at 0.1° spatial resolution spanning from 2001 to 2024. ERA5-Land represents the fifth iteration of the European Center for Medium-Range Weather Forecasts atmospheric reanalysis dataset and provides comprehensive global climate information. This dataset integrates model-derived data with extensive global observational records, resulting in a comprehensive and harmonized global meteorological dataset.

2.2. FluxSat GPP product

GPP data were adopted from FluxSat GPP version 2.2 product (Joiner and Yoshida 2020). We used FluxSat GPP v2.2, spanning 2001–2024, and resampled it from 0.05° to 0.1° spatial resolution.

FluxSat GPP was derived using a machine learning method with the collection of 6.1 MCD43C Bidirectional Reflectance Distribution Function-Adjusted Reflectance on the NASA Terra and Aqua satellites trained on FLUXNET2015 and OneFlux data. The FluxSat GPP dataset demonstrates good quality and agreement with eddy covariance flux measurements and has been validated in numerous studies (Zhao *et al* 2023, Wang *et al* 2023b).

2.3. Near-infrared reflectance of terrestrial vegetation (NIR_v)

Near-infrared reflectance of terrestrial vegetation (NIR_v) is highly correlated with solar-induced chlorophyll fluorescence, a metric used to estimate global gridded GPP magnitudes (Badgley *et al* 2017). NIR_v was calculated as follows:

$$\mathrm{NIR_v} = (NDVI - 0.08) \times NIR \tag{1}$$

where *NDVI* is the monthly normalized difference vegetation index (NDVI) and *NIR* is the monthly surface reflectance in the near-infrared (841–876 nm).

NDVI data were adopted from the Moderate-Resolution Imaging Spectroradiometer (MODIS) MOD13C2 Version 6.1 product (Didan 2021). MOD13C2 provides NDVI, enhanced vegetation index, VI QA, reflectance data, angular information, and spatial statistics at a 0.05° climate modeling grid resolution. We retained the NDVI and NIR reflectance data for analysis with a QA flag of 0 (Good Data) and 1 (Marginal Data) and resampled them to a 0.1° resolution.

2.4. MODIS landcover product

Land-cover data were obtained from the MODIS Land Cover Climate Modeling Grid Product (MCD12C1), which provides a spatially aggregated and reprojected version of the tiled MCD12Q1 product (Friedl and Sulla-Menashe 2022). The product provides global land cover maps of the International Geosphere (Biosphere) and University of Maryland classification schemes at an annual spatial resolution of 0.05° from 2001 to 2022. We applied land cover data from the IGBP classification for 2022 and resampled the data to a resolution of 0.1°.

2.5. Anomalies and contributions

We calculated anomalies in climate- and vegetation-related variables from 2001 to 2024 using the following two steps. First, the monthly average values of climate- and vegetation-related variables were computed for each pixel

$$\overline{V(t)} = \frac{1}{n}\sum\nolimits_{1}^{n} V(t) \tag{2}$$

where $V(t)$ is the annual climate- or vegetation-related variables for the corresponding month, $\overline{V(t)}$ is the average value of the monthly climate- or vegetation-related variables from 2001 to 2024, t is the corresponding month, and n is the number of years from 2001 to 2024.

The anomalies of climate- and vegetation-related variables for each month from 2001 to 2024 were then derived by subtracting the corresponding monthly average values from the monthly data:

$$V_{\mathrm{anom}}(t) = V(t) - \overline{V(t)} \tag{3}$$

where $V_{\mathrm{anom}}(t)$ is the anomalies of climate- and vegetation-related variables.

Based on the anomalies in air temperature, precipitation, and GPP, we identified the period of HD2023 as September, 2023 to January, 2024 (figure S1 in supplementary material). Therefore, we defined the study period as September to January of each year, calculating anomalies of climate- and vegetation-related variables (i.e. GPP and NIR_v) for the Amazon. Additionally, we detrended the anomalies with the trend calculated from the variations in the period 2001–2024 to eliminate the influence of human management, CO_2 fertilization, and other factors (Sitch *et al* 2015, Yang *et al* 2022).

Finally, we quantitatively estimated the individual contributions of temperature, solar radiation downwards, and soil moisture to GPP and NIR_v anomalies in different vegetation types using a simple decomposition method, which have been widely used in previous studies (Piao *et al* 2013, Jung *et al* 2017):

$$y = \beta^{\mathrm{T}}\Delta\mathrm{T} + \beta^{\mathrm{SRD}}\Delta\mathrm{SRD} + \beta^{\mathrm{SM}}\Delta\mathrm{SM} + \varepsilon \tag{4}$$

where y is the annual anomalies of GPP and NIR_v for different vegetation types according to the MCD12C1 land cover map for 2022, which are mainly evergreen broadleaf forest, savanna, and grassland; ΔT, ΔSRD, and ΔSM are the annual anomalies of temperature, solar radiation downwards, and soil moisture, respectively; β^{T}, β^{SRD}, and β^{SM} are the apparent sensitivities of temperature, solar radiation downwards, and soil moisture; and ε is the residual term.

3. Results

3.1. Anomalies of climate and vegetation photosynthesis since 2001

Under the influence of a strong El Niño event in 2023, the Amazon suffered from widespread high temperatures and drought events from September 2023 to January 2024 (HD2023). The Amazon experienced the largest positive anomaly in air temperature (1.13 ± 0.30 °C) and largest negative anomaly in precipitation (−29.51 ± 7.57 mm) since 2001 (figure 1(a)). Due to reduced precipitation and decreased cloud cover, there was also a strong positive anomaly in solar radiation downwards (7.78 ± 3.83 W m^{-2}) during HD2023 (figure 1(b)). Therefore, increased evapotranspiration caused by high air temperature and intensive radiation,

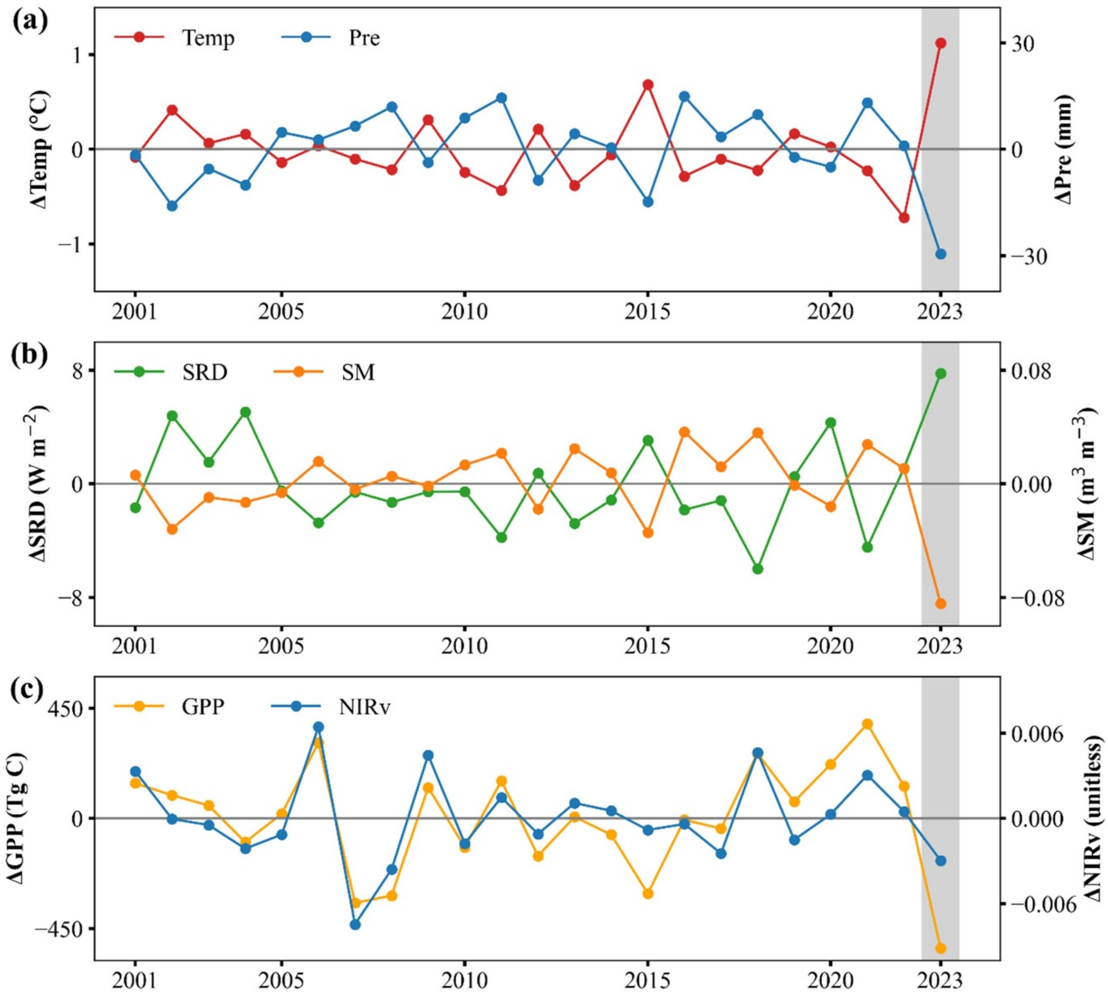

Figure 1. Detrended anomalies in climate and photosynthesis during September–January from 2001 to 2024. Time series of anomalies in (a) 2 m air temperature (ΔTemp) and precipitation (ΔPre), (b) solar radiation downwards (ΔSRD) and soil moisture (ΔSM) anomalies, and (c) gross primary productivity (ΔGPP) and near-infrared reflectance of vegetation (ΔNIR_v) during September–January from 2001 to 2024 averaged in Amazon.

coupled with reduced precipitation and accelerated soil moisture depletion, exacerbates drought conditions. The soil moisture over the Amazon during HD2023 showed a reduction of 0.08 ± 0.03 m^3 m^{-3} (figure 1(b)).

Abnormally high air temperatures and soil dryness have a serious impact on terrestrial ecosystems. During HD2023, the interactions between air temperature, precipitation, solar radiation downwards, and soil moisture greatly influenced photosynthesis in the Amazon. GPP severely declined by 530 Tg C, marking the most severe reduction observed since 2001 (figure 1(c)). The interannual variability in NIR_v was generally consistent with that of GPP, although the decrease in NIR_v was less severe, possibly because of the influence of cloud cover and soil reflectance.

3.2. Spatial distribution of anomalies in climate and vegetation photosynthesis

As expected, the anomalies in climate and vegetation photosynthesis showed clear spatiotemporal heterogeneity. During HD2023, seriously high temperature and low precipitation anomalies were observed in the Amazon region. Over 80% of Amazon experienced a positive temperature anomaly exceeding 1 °C (figure 2(a)), whereas approximately 60% of the area witnessed a reduction in precipitation of more than 30 mm (figure 2(b)). The entire Amazon received strong solar radiation (figure 2(c)). Soil moisture anomalies were most severe in the central Amazon (figure 2(d)), persisting from September to November. However, the spatial distribution of the GPP anomalies did not fully align with that of the climate anomalies. Most areas experienced a decline in the GPP to varying extents (figure 2(e)). The regions with the most severe relative declines were the grasslands of the east and savannas of the south, while the decrease in GPP for evergreen broadleaf forests in the central region remained within 10%. The spatial pattern of NIR_v changes was similar to that of GPP, with the most severe relative declines occurring in the grasslands of the east and savannas of the south (figures 2(e) and (f)). However, in the central region of the evergreen broadleaf forests, the changes

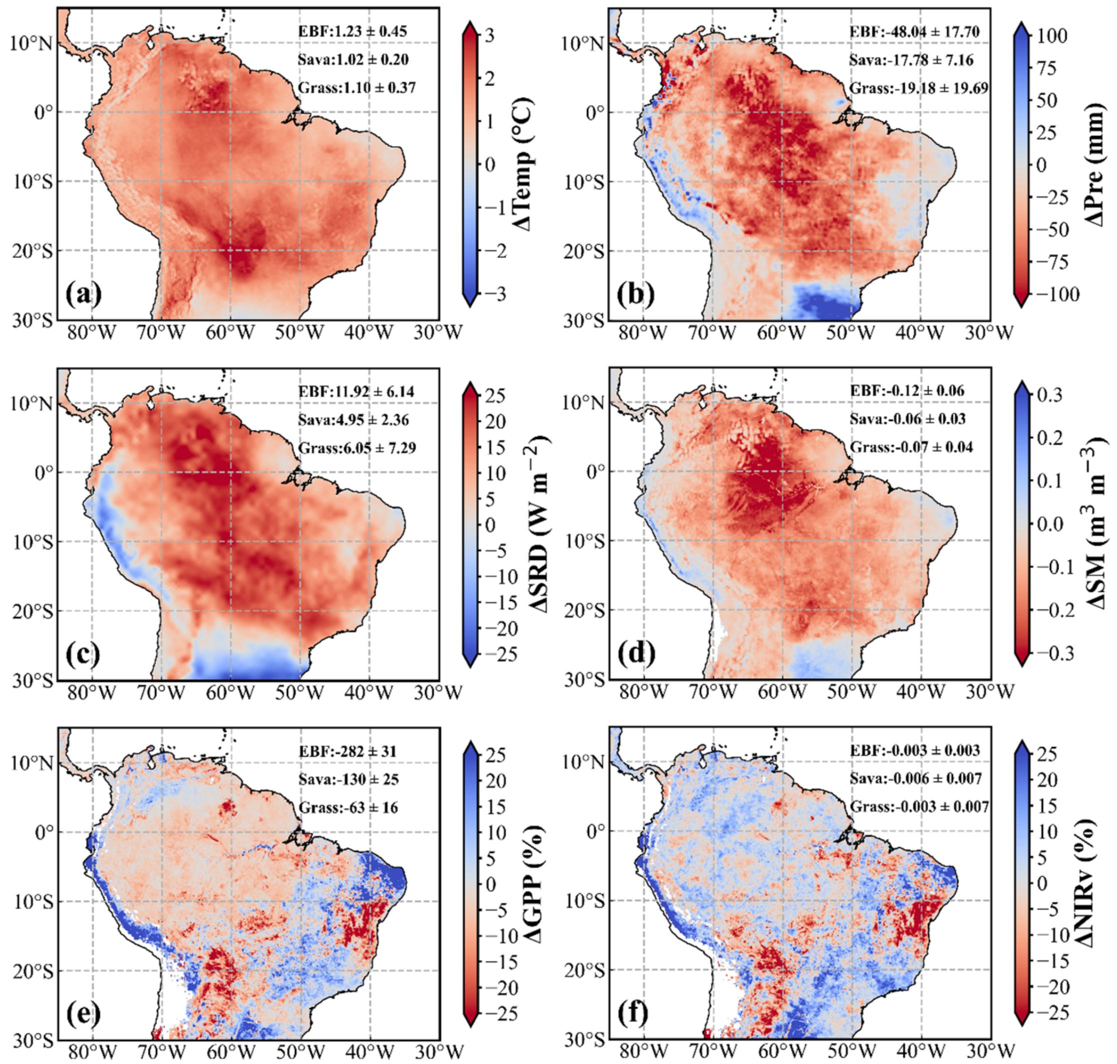

Figure 2. Spatial distributions of the anomalies for (a) 2 m air temperature, (b) precipitation, (c) solar radiation downwards, and (d) soil moisture and relative changes (%) in (e) GPP and (f) NIR_v during September–January from 2001 to 2024. The text in (a–f) show the average changes in Temp (°C), Pre (mm), SRD (W m^{-2}), SM (m^3 m^{-3}), NIR_v (unitless), and the total carbon flux for GPP (Tg C) over the evergreen broadleaf forest (EBF), savanna (Sava), and grassland (Grass) during HD2023 over Amazon, respectively.

in NIR_v differed from those in GPP, suggesting a weaker correlation between NIR_v and GPP in evergreen broadleaf forests (figures 2(e) and (f)).

There are three major vegetation types in the Amazon: evergreen broadleaf forest (42%), savanna (28%), and grassland (20%) (Fig. S3(a) in supplementary material). The average NIR_v anomalies for these vegetation types were all negative, with the lowest value being −0.006 for savanna, followed by −0.003 for both evergreen broadleaf forest and grassland (figure 2(f)). In comparison, evergreen broadleaf forest contributed the most to the total anomaly in GPP, with a value of −282.49 Tg C, accounting for approximately 53% of the total decrease in GPP across the region. The second was savanna, exhibiting an anomaly of −130.20 Tg C, while grassland contributed the least, with an anomaly of −63.08 Tg C (figure 2(e)).

To better understand the development of HD2023 and its impact on vegetation photosynthesis, we mapped the spatial patterns of the anomalies in climate- and vegetation-related variables on a monthly basis (figure S2 in supplementary material). Overall, the spatial pattern of HD2023, as observed through the distribution of various meteorological factors, showed a gradual spread from northwest to southeast. However, owing to differences in vegetation types, the response of terrestrial ecosystems to drought exhibited variable spatiotemporal patterns.

3.3. Contribution of environmental factors to the photosynthetic anomalies

Using a multiple linear regression analysis, we sought to understand the contributions of air temperature, solar radiation downwards, and soil moisture to anomalies in GPP and NIR_v across different vegetation types in the Amazon. The overall accuracy of the model was satisfactory (R^2: 0.30–0.49), with all models being significant at the 95% confidence level

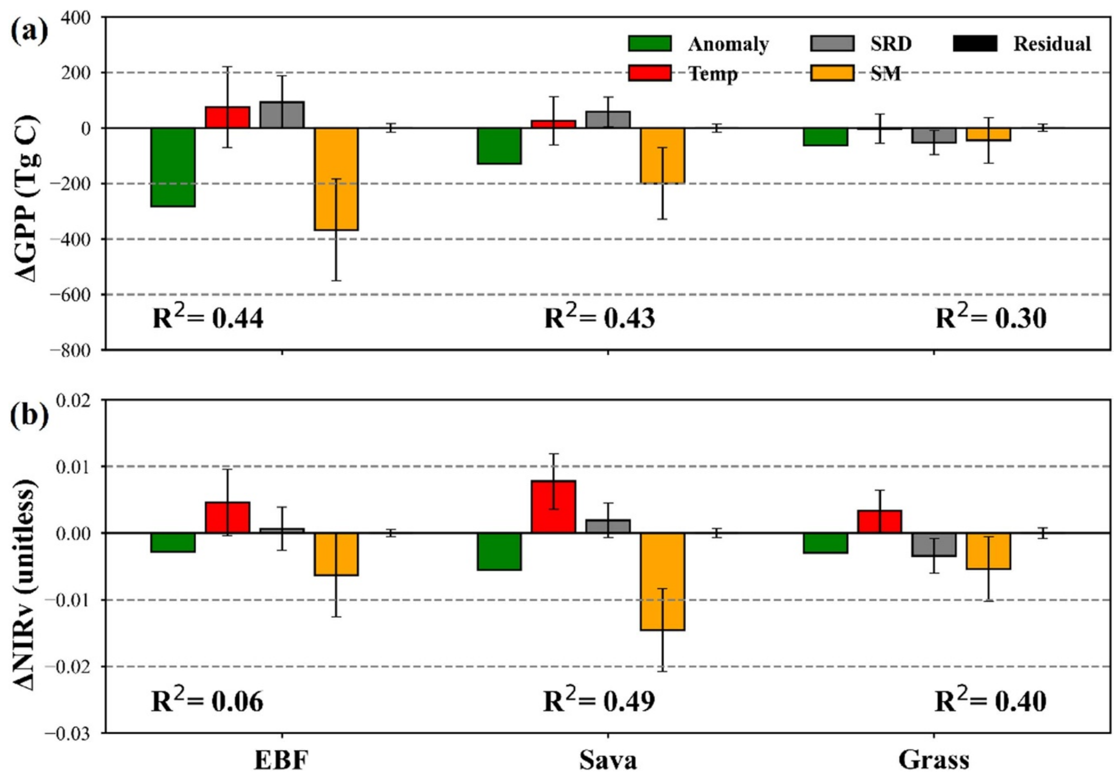

Figure 3. Contributions of Temp, SRD, and SM to anomalies of (a) GPP and (b) NIR_v over different vegetation types in the Amazon. The term 'residual' denotes the unexplained variation and the error bars represent the standard error.

($p < 0.05$). However, the attribution of NIR_v anomalies in the evergreen broadleaf forest still exhibited poor performance ($R^2 = 0.06$).

In terms of GPP and NIR_v, a reduction in soil moisture predominantly drove a decline in photosynthesis across all three vegetation types. (figures 3(a) and (b)), agreeing with the results of previous studies (Meir *et al* 2015, Liu *et al* 2020). For evergreen broadleaf forest and savanna, high solar radiation appeared to promote photosynthesis (figures 3(a) and (b)). This suggests that high solar radiation partially offsets the negative effects of water stress on photosynthesis. Li *et al* (2018) investigated the impact of the 2015 drought on photosynthesis in the Amazon rainforest using satellite solar-induced chlorophyll fluorescence products along with other climate and vegetation datasets and reached similar conclusions. Intense solar radiation suppressed photosynthesis in grassland. Grassland typically has shallow root systems and intense solar radiation accelerates soil evaporation, preventing them from replenishing sufficient moisture. Finally, higher temperatures seemed to promote photosynthesis in evergreen broadleaf forest and savanna.

3.4. Progress of HD2023 and the response of vegetations to HD2023

HD2023 lasted for 5 months (September 2023 to January 2024), severely affecting the vegetation GPP in the Amazon. Overall, the progress can be chronologically divided into four stages (figure 4). First, in the early stage (September 2023), despite positive anomaly (+0.86 °C) in air temperature and negative anomalies in precipitation (−18.00 mm) and SM (−0.049 m^3 m^{-3}), GPP still exhibited a slightly positive anomaly (+20.3 Tg C). This indicated that GPP had not been suppressed yet, even if HD2023 started at this early stage.

In the middle stage (October and November 2023), positive anomalies (+1.36 °C and +1.52 °C) in air temperature, along with negative anomalies in precipitation (−34.00 mm and −45.48 mm), resulted in negative anomalies in SM (−0.096 m^3 m^{-3} and −0.128 m^3 m^{-3}). Meantime, GPP exhibited negative anomalies (−37.4 Tg C and −140.5 Tg C). It indicated that HD2023 started to suppress GPP in Amazon at this stage.

In the late stage (December 2023), the positive anomaly in air temperature (+1.07 °C) decreased and the negative anomaly in precipitation (−31.64 mm) decreased, resulting to smaller negative anomaly in SM (−0.097 m^3 m^{-3}) compared to the previous stage. In this stage, the negative anomaly in GPP (−153.7 Tg C) was larger than that in previous stage. It indicated that the suppress of GPP still proceeded even if HD2023 entered to the late stage (figure 4).

In the end stage (January 2024), the positive anomaly in air temperature (+0.81 °C) and the

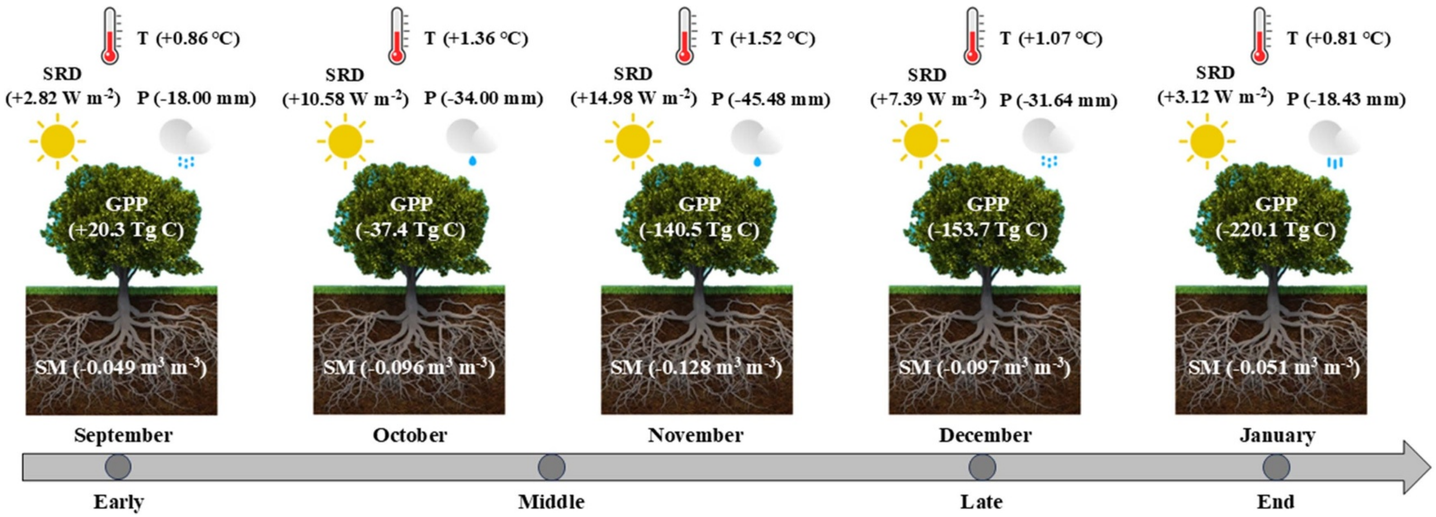

Figure 4. Progress of detrended anomalies of monthly GPP and environmental variables in the Amazon during HD2023 (September 2023 to January 2024). T, P, SRD, SM, and GPP denote the detrended anomalies in 2 m air temperature, precipitation, solar radiation downwards, soil moisture, and gross primary productivity, respectively. Total GPP loss caused by HD2023 is −530 Tg C for 5 months (September 2023 to January 2024).

negative anomaly in precipitation (−18.43 mm) both further decreased compared to those of the previous stage. The negative anomaly in SM was small (−0.051 m^3 m^{-3}), indicating the end of HD2023. However, the negative anomaly in GPP became more severe (−220.1 Tg C) compared to that of the previous stage. It indicated that the suppress of GPP further proceeded even if HD2023 was close to the end.

To investigate variations in the responses of different vegetation types to HD2023, we selected a region of interest for each vegetation type, each covering an area of 1° longitude × 1° latitude (figure S3(a) in supplementary material). The monthly relative changes in $\Delta GPP/\overline{GPP}$ for EBF were small (<10%) during HD2023 (figure S3(b)), indicating that the impacts of HD2023 on GPP of EBF was small. In contrast, the monthly $\Delta GPP/\overline{GPP}$ for Sava were −14%, −28%, −9%, and −11% during October 2023 to January 2024 (figure S3(b)), indicating that the Sava GPP affected by the HD2023 event. Also, the monthly $\Delta GPP/\overline{GPP}$ for Grass were in the range of −40% to −75% during September to December 2023, and it recovered to 55% in January 2024 (figure S3(b). The impacts of the HD2023 event on Grass GPP was the most severe among the three vegetation types during September to December 2023. Therefore, the sensitivity to the HD2023 event among the three vegetation types can be ranked as follows: grassland, savanna, and evergreen broadleaf forest.

4. Discussion

4.1. Progress of HD2023 and GPP responses

The asynchronism in the progress of HD2023 and GPP responses revealed that at least 1 month of lag existed between GPP responses and HD2023 (figure 4). Specifically, heatwaves are usually associated with a high vapor pressure deficit, which causes the decrease in stomatal conductance, suppressing photosynthesis rates (Merilo *et al* 2018, Hsu *et al* 2021). During the progress of prolonged drought, leaf photosynthetic capacity (i.e. V_{cmax25}) and synthesis of leaf photosynthetic pigments (i.e. chlorophyll and carotenoid) would be damaged with accumulated soil water deficit, resulting to further suppression in GPP (Chen *et al* 2019a, Li *et al* 2024b). Although climate conditions in the Amazon almost returned to normal in January 2024, GPP was still severely suppressed. This could be attributed to spatial heterogeneity of climate conditions in the Amazon region and the diverse responses of GPP among EBF, Sava and Grass. This issue will be clarified in detail in the next section.

4.2. Response of different vegetation types to HD2023

The EBF is located in the tropical rainforest (Af) climate zones (Beck *et al* 2023). The Af region usually receives abundant rainfall throughout the year and the rooting depth of tropical rain forests can reach 3–4 m depths (Jackson *et al* 1996, Bachofen *et al* 2024). Thus, the availability of soil moisture to EBF were still good enough for maintaining photosynthesis even if $\Delta Pre/\overline{Pre}$ was −80% (figure S3(c)) and $\Delta SM/\overline{SM}$ was around −40% in October (figure S3(d)) during the HD2023. The Sava was a transition vegetation type between forests and grassland, with both trees and grass. The Sava is located in the tropical savannah (Aw) climate zones with distinct wet and dry seasons (Beck *et al* 2023). The precipitation and SM deficit during October to November 2023 (figure S3(d)) would suppress the photosynthesis of grass, which is more sensitive to SM deficit. Trees would shift root water uptake from surface to deeper soil layers during the progress of SM dry-down (Bachofen *et al* 2024). Also, tropical trees have stem water storage, which could serve as a buffer to drought (Preisler *et al* 2022). Thus, impacts of the HD2023 event to trees in Sava could be small. Grass is low-growing vegetation. Under drought conditions, the photosynthesis of such vegetation is highly sensitive to SM availability. Also, the shallower roots of tropical grass in Grass than those of trees limit its ability to access deep soil moisture (Gao *et al* 2024), which could be another reason why the most severe photosynthesis suppress occurred in Grass.

4.3. Comparison with previous droughts since 2000

HD2023 in the Amazon region garnered widespread attention (Espinoza *et al* 2024, Meunier *et al* 2024, Wagner *et al* 2024). Our findings on HD2023 revealed a GPP reduction of 530 Tg C across the region, marking the most severe decline in the past 20 years.

Compared with previous drought events, our results show consistency in that extreme droughts led to substantial carbon losses in the Amazon region. However, our study revealed that the decline in GPP caused by HD2023 was the most severe since the beginning of the 21st century. However, when considering carbon loss alone, it did not appear to be the most severe factor compared with previous droughts (table 1). This discrepancy can be explained by differences in the methods, duration of drought events, and scope of the study. First, there were notable methodological differences. Previous studies primarily relied on forest plots and model simulations, both of which are subject to considerable uncertainty (Holdaway *et al* 2014, Post *et al* 2018). In contrast, the FluxSat GPP product, which combines satellite and flux tower data using machine learning techniques, has been increasingly adopted to assess regional carbon uptake (Lee *et al* 2022) and the impact of extreme climatic events on the terrestrial carbon cycle (Byrne *et al* 2021, Wang *et al* 2023a). Second, the duration of drought events varies across studies. For instance, Phillips *et al* examined the 2005 drought on an annual scale, whereas other studies, including ours, defined

Table 1. Previous droughts in the Amazon since 2000.

Events	Method	Duration	Carbon loss	References
2005 drought	Permanent forest plots	2005.1–2005.12	1.2–1.6 Pg C	(Phillips *et al* 2009)
2010 drought	Forest plots	2010.5–2010.12	0.23–0.53 Pg C	(Doughty *et al* 2015)
2015–2016 drought	Land surface model (LSM)	2015.10–2016.3	0.95 Pg C	(van Schaik *et al* 2018)
2023–2024 drought	Machine learning	2023.9–2024.1	0.53 Pg C	This study

specific start and end dates of the drought periods. Finally, there were differences in the geographical scopes of the studies. Most studies have focused on the biogeographical Amazon region, whereas our study covers a broader area. Consequently, regions unaffected by drought may have offset some of their observed carbon losses.

Notably, the frequency of CHWDs is expected to increase in the future owing to global warming (Ridder *et al* 2022). Therefore, further research on the response mechanisms of ecosystems in the Amazon to CHWDs is required to better understand the ecosystem impacts caused by these occurrences. Notably, our research showed that a decline in soil moisture was the main factor driving the decrease in GPP during HD2023. Therefore, future studies on the response of vegetation in the Amazon to CHWDs should focus on changes in soil moisture. Additionally, given the variability in vegetation types in the Amazon, it is important to consider the different thresholds of soil moisture for various vegetation types.

5. Conclusions

We conducted an in-depth analysis of the impact of HD2023 on vegetation photosynthesis and its developmental processes in the Amazon. HD2023 have resulted in severe temperature, precipitation, solar radiation, and soil moisture anomalies since the beginning of the 21st century. Anomalies in these climatic factors have led to a widespread decline in photosynthesis in the Amazon. Specifically, HD2023 caused a severe decline in total GPP of 530 Tg C and average NIR_v of 0.003.

HD2023 lasted 5 months (September 2023 to January 2024). During the early and middle phases, persistently high temperatures and a lack of precipitation led to a continuous decline in soil moisture, severely impacting plant photosynthesis and causing a sustained reduction in GPP. In the late phase, despite a slight easing of meteorological conditions, the cumulative effects of drought and delayed response of vegetation resulted in the most severe GPP decline in January. Across spatial scales, HD2023 began in the northwestern evergreen broadleaf forest and gradually spread southeast across the entire region. The two datasets reflecting vegetation photosynthesis, FluxSat GPP, and MODIS NIR_v, showed strong overall spatial consistency but weaker consistency in the evergreen broadleaf forest region.

The dominant climatic factors influencing photosynthetic anomalies were consistent across the different vegetation types. Multiple linear regression analysis indicated that the decrease in photosynthesis across the three vegetation types was primarily attributable to reduced soil moisture. Additionally, in evergreen broadleaf forests and savannas, high solar radiation partially mitigates the adverse effects of water stress on photosynthesis. Different vegetation types exhibited varying sensitivities to CHWD, ranking as grassland > savanna > evergreen broad forest.

Overall, our research identified a CHWD event in the Amazon region during 2023–2024 and evaluated its impact on the GPP. We revealed the roles of various environmental factors and the differential responses of vegetation types to extreme climatic events, providing valuable insights for ecosystem management and climate change adaptation strategies.

Data availability statement

All reanalysis and satellite data used in this study are publicly available at the following URLs:

(1) 0.1° ERA5-Land monthly averaged dataset: https://cds.climate.copernicus.eu/datasets/reanalysis-era5-land-monthly-means?tab=overview.
(2) 0.05° FluxSat GPP version 2.2 product: https://avdc.gsfc.nasa.gov/pub/tmp/FluxSat_GPP/ .
(3) 0.05° MODIS NDVI product (MOD13C2 Version 6.1): https://lpdaac.usgs.gov/products/mod13c2v061/.
(4) 0.05° MODIS Land Cover Climate Modeling Grid Product (MCD12C1 Version 6.1): https://lpdaac.usgs.gov/products/mcd12c1v061/.

All data that support the findings of this study are included within the article (and any supplementary files).

Acknowledgment

This research was funded by the National Key Research and Development Program from Ministry of Science and Technology, China (2023YFB3907402) and the National Natural Science Foundation of China (Grant Nos. 42261144754 and 42250205).

ORCID iDs

Te Yang https://orcid.org/0009-0001-5636-8221
Bin Chen https://orcid.org/0000-0002-1042-5649
Xiyan Xu https://orcid.org/0000-0003-2732-1325
Paulo Artaxo https://orcid.org/0000-0001-7754-3036

References

Artaxo P *et al* 2022a Tropical and boreal forest–atmosphere interactions: a review *Tellus* B **24** 24–163
Artaxo P 2023 Amazon deforestation implications in local/regional climate change *Proc. Natl Acad. Sci.* **120** e2317456120
Artaxo P, Hansson H C, Machado L A T and Rizzo L V 2022b Tropical forests are crucial in regulating the climate on Earth *PLOS Clim.* **1** e0000054
Bachofen C, Tumber-Dávila S J, Mackay D S, McDowell N G, Carminati A, Klein T, Stocker B D, Mencuccini M and Grossiord C 2024 Tree water uptake patterns across the globe *New Phytol.* **242** 1891–910
Badgley G, Field C B and Berry J A 2017 Canopy near-infrared reflectance and terrestrial photosynthesis *Sci. Adv.* **3** e1602244
Bastos A *et al* 2020 Direct and seasonal legacy effects of the 2018 heat wave and drought on European ecosystem productivity *Sci. Adv.* **6** eaba2724
Beck H E, McVicar T R, Vergopolan N, Berg A, Lutsko N J, Dufour A and Miralles D G 2023 High-resolution (1 km) Köppen-Geiger maps for 1901–2099 based on constrained CMIP6 projections *Sci. Data* **10** 724
Bennett A C *et al* 2023 Sensitivity of South American tropical forests to an extreme climate anomaly *Nat. Clim. Change* **13** 967–74
Byrne B *et al* 2021 The carbon cycle of southeast Australia during 2019–2020: drought, fires, and subsequent recovery *AGU Adv.* **2** e2021AV000469
Chen B, Chen J M, Baldocchi D D, Liu Y, Wang S, Zheng T and Croft H 2019a Including soil water stress in process-based ecosystem models by scaling down maximum carboxylation rate using accumulated soil water deficit *Agric. For. Meteorol.* **276** 107649
Chen B, Xu X, Wang S, Yang T, Liu Z and Falk S 2024 Carbon dioxide fertilization enhanced carbon sink offset by climate change and land use in Amazonia on a centennial scale *Sci. Total Environ.* **955** 176903
Chen W *et al* 2019b Negative extreme events in gross primary productivity and their drivers in China during the past three decades *Agric. For. Meteorol.* **275** 47–58
Davidson E A *et al* 2012 The Amazon basin in transition *Nature* **481** 321–8
Didan K 2021 MODIS/Terra vegetation indices monthly L3 global 0.05 Deg CMG V061 [Data set] *NASA EOSDIS Land Processes Distributed Active Archive Center* (https://doi.org/10.5067/MODIS/MOD13C2.061) (Accessed 12 February 2025)
Doughty C E *et al* 2015 Drought impact on forest carbon dynamics and fluxes in Amazonia *Nature* **519** 78–U140
Espinoza J C, Jimenez J C, Marengo J A, Schongart J, Ronchail J, Lavado-Casimiro W and Ribeiro J V M 2024 The new record of drought and warmth in the Amazon in 2023 related to regional and global climatic features *Sci. Rep.* **14** 8107
Feng Y *et al* 2024 Global patterns and drivers of tropical aboveground carbon changes *Nat. Clim. Change* **14** 1064–70
Friedl M and Sulla-Menashe D 2022 MODIS/Terra+Aqua Land Cover Type Yearly L3 Global 0.05Deg CMG V061 [Data set] (https://doi.org/10.5067/MODIS/MCD12C1.061) (Accessed 12 February 2025)
Gampe D, Zscheischler J, Reichstein M, O'Sullivan M, Smith W K, Sitch S and Buermann W 2021 Increasing impact of warm droughts on northern ecosystem productivity over recent decades *Nat. Clim. Change* **11** 772–9
Gao H, Hrachowitz M, Wang-Erlandsson L, Fenicia F, Xi Q, Xia J, Shao W, Sun G and Savenije H H 2024 Root zone in the Earth system *Hydrol. Earth Syst. Sci.* **28** 4477–99
Holdaway R J, McNeill S J, Mason N W and Carswell F E 2014 Propagating uncertainty in plot-based estimates of forest carbon stock and carbon stock change *Ecosystems* **17** 627–40
Hsu P-K, Takahashi Y, Merilo E, Costa A, Zhang L, Kernig K, Lee K H and Schroeder J I 2021 Raf-like kinases and receptor-like (pseudo) kinase GHR1 are required for stomatal vapor pressure difference response *Proc. Natl Acad. Sci.* **118** e2107280118
Jackson R B, Canadell J, Ehleringer J R, Mooney H A, Sala O E and Schulze E-D 1996 A global analysis of root distributions for terrestrial biomes *Oecologia* **108** 389–411
Jiang N *et al* 2024 Enhanced risk of record-breaking regional temperatures during the 2023–24 El Niño *Sci. Rep.* **14** 2521
Jiménez-Muñoz J C, Mattar C, Barichivich J, Santamaria-Artigas A, Takahashi K, Malhi Y, Sobrino J A and Schrier G V D 2016 Record-breaking warming and extreme drought in the Amazon rainforest during the course of El Nino 2015–2016 *Sci. Rep.* **6** 33130
Joiner J and Yoshida Y 2020 Satellite-based reflectances capture large fraction of variability in global gross primary production (GPP) at weekly time scales *Agric. For. Meteorol.* **291** 108092
Jung M *et al* 2017 Compensatory water effects link yearly global land CO_2 sink changes to temperature *Nature* **541** 516–20
Lee E, Koster R D, Ott L E, Joiner J, Zeng F W, Kolassa J, Reichle R H, Arsenault K R, Hazra A and Shukla S 2022 Skillful seasonal forecasts of land carbon uptake in Northern mid-and high latitudes *Geophys. Res. Lett.* **49** e2021GL097117
Li T *et al* 2024a Widespread reduction in gross primary productivity caused by the compound heat and drought in Yangtze River Basin in 2022 *Environ. Res. Lett.* **19** 034048
Li X, Xiao J and He B 2018 Higher absorbed solar radiation partly offset the negative effects of water stress on the photosynthesis of Amazon forests during the 2015 drought *Environ. Res. Lett.* **13** 044005
Li X, Zhang W, Niu D and Liu X 2024b Effects of abiotic stress on chlorophyll metabolism *Plant Sci.* **342** 112030
Littell J S, Peterson D L, Riley K L, Liu Y Q and Luce C H 2016 A review of the relationships between drought and forest fire in the United States *Glob. Change Biol.* **22** 2353–69
Liu L B, Gudmundsson L, Hauser M, Qin D H, Li S C and Seneviratne S I 2020 Soil moisture dominates dryness stress on ecosystem production globally *Nat. Commun.* **11** 4892
Meir P, Wood T E, Galbraith D R, Brando P M, Da Costa A C L, Rowland L and Ferreira L V 2015 Threshold responses to soil moisture deficit by trees and soil in tropical rain forests: insights from field experiments *BioScience* **65** 882–92
Merilo E, Yarmolinsky D, Jalakas P, Parik H, Tulva I, Rasulov B, Kilk K and Kollist H 2018 Stomatal VPD response: there is more to the story than ABA *Plant Physiol.* **176** 851–64
Meunier F *et al* 2024 The impact of the 2023–2024 drought on intact Amazon forests' productivity (https://doi.org/10.21203/rs.3.rs-4705191/v1)
Muñoz-Sabater J *et al* 2021 ERA5-Land: a state-of-the-art global reanalysis dataset for land applications *Earth Syst. Sci. Data* **13** 4349–83
Pan Y D *et al* 2011 A large and persistent carbon sink in the world's forests *Science* **333** 988–93

Perkins S E, Alexander L and Nairn J 2012 Increasing frequency, intensity and duration of observed global heatwaves and warm spells *Geophys. Res. Lett.* **39** L20714
Perkins-Kirkpatrick S, Barriopedro D, Jha R, Wang L, Mondal A, Libonati R and Kornhuber K 2024 Extreme terrestrial heat in 2023 *Nat. Rev. Earth Environ.* **5** 244–6
Phillips O L *et al* 2009 Drought sensitivity of the Amazon rainforest *Science* **323** 1344–7
Piao S *et al* 2013 Evaluation of terrestrial carbon cycle models for their response to climate variability and to CO_2 trends *Glob. Change Biol.* **19** 2117–32
Post H, Hendricks Franssen H-J, Han X, Baatz R, Montzka C, Schmidt M and Vereecken H 2018 Evaluation and uncertainty analysis of regional-scale CLM4.5 net carbon flux estimates *Biogeosciences* **15** 187–208
Preisler Y, Hölttä T, Grünzweig J M, Oz I, Tatarinov F, Ruehr N K, Rotenberg E and Yakir D 2022 The importance of tree internal water storage under drought conditions *Tree Physiol.* **42** 771–83
Ridder N N, Ukkola A M, Pitman A J and Perkins-Kirkpatrick S E 2022 Increased occurrence of high impact compound events under climate change *npj Clim. Atmos. Sci.* **5** 3
Rodrigues M 2023 The Amazon's record-setting drought: how bad will it be? *Nature* **623** 675–6
Sitch S *et al* 2015 Recent trends and drivers of regional sources and sinks of carbon dioxide *Biogeosciences* **12** 653–79
Stríkis N M *et al* 2024 Modern anthropogenic drought in Central Brazil unprecedented during last 700 years *Nat. Commun.* **15** 1728
van Schaik E, Killaars L, Smith N E, Koren G, Van Beek L, Peters W and van der Laan-luijkx I T 2018 Changes in surface hydrology, soil moisture and gross primary production in the Amazon during the 2015/2016 El Niño *Phil. Trans. R. Soc.* B **373** 20180084
Wagner F H, Favrichon S, Dalagnol R, Hirye M C, Mullissa A and Saatchi S 2024 The Amazon's 2023 drought: Sentinel-1 reveals extreme Rio Negro River contraction *Remote Sens.* **16** 1056
Wang J *et al* 2023a Unprecedented decline in photosynthesis caused by summer 2022 record-breaking compound drought-heatwave over Yangtze River Basin *Sci. Bull.* **68** 2160–3
Wang M, Wang S, Wang J, Yan H, Mickler R A, Shi H, He H, Huang M and Zhou L 2018 Detection of positive gross primary production extremes in terrestrial ecosystems of China during 1982–2015 and analysis of climate contribution *J. Geophys. Res.* **123** 2807–23
Wang Y, Liu J J, Wennberg P O, He L Y, Bonal D, Köhler P, Frankenberg C, Sitch S and Friedlingstein P 2023b Elucidating climatic drivers of photosynthesis by tropical forests *Glob. Change Biol.* **29** 4811–25
Yang J, Tian H Q, Pan S F, Chen G S, Zhang B W and Dangal S 2018 Amazon drought and forest response: largely reduced forest photosynthesis but slightly increased canopy greenness during the extreme drought of 2015/2016 *Glob. Change Biol.* **24** 1919–34
Yang R *et al* 2022 Divergent historical GPP trends among state-of-the-art multi-model simulations and satellite-based products *Earth Syst. Dyn.* **13** 833–49
Zhao D Y, Zhang Z Y and Zhang Y G 2023 Soil moisture dominates the forest productivity decline during the 2022 China compound drought-heatwave event *Geophys. Res. Lett.* **50** e2023GL104539
Zhu X, Zhang S, Liu T and Liu Y 2021 Impacts of heat and drought on gross primary productivity in China *Remote Sens.* **13** 378
Zscheischler J *et al* 2014 A few extreme events dominate global interannual variability in gross primary production *Environ. Res. Lett.* **9** 035001